Computer Life (CPL) ISSN: 1819-4818
DELIVERING QUALITY SCIENCE TO THE WORLD

Optimization of Thermal Flow Field of Armored Vehicle Power Cabin and Its Comprehensive Evaluation

Jun Lu [a], Qingguo Luo * and Yao Zhao

Vehicle Engineering Department, Army Academy of Armored Forces, Beijing China.

[a]872430579@qq.com, [c]lqg_zgy@163.com, *****421834459@qq.com.

Abstract: In this paper, a closed-type power cabin is taken as an example to establish a CFD model for the outer wall of the Power transmission device, and numerical analysis is carried out. In view of the problem of excessive heat load in the power cabin of the tank, a hole is opened above the armored deck of the power cabin and a ventilation fan is added. The size, position, number and arrangement of the fan are not affected by the overall structure of the power cabin and the heat dissipation. The size of the air gap has changed. Finally, the airway is comprehensively evaluated by the combination of entropy method and subordination degree linear weighted programming method. The application example shows that the temperature of the main high temperature components in the power cabin is effectively reduced. The comprehensive evaluation method is effective and feasible.
Keywords: Power cabin, Cooling wind tunnel, CFD, Structural optimization, Comprehensive evaluation.

1. INTRODUCTION

The armored vehicle power cabin is the "core" of the armored vehicle. It is equipped with high temperature components such as power transmission device, cooling system, intake and exhaust system. With the continuous improvement of the engine rate, the new heat source of the motor and high-temperature battery is added and the power cabin is advanced. The layout of the integrated design leads to an increase in the thermal load in the cabin and a deterioration in the temperature environment [1]. Therefore, the cooling of the power cabin has become an important factor affecting the overall performance of the vehicle [2].

The armored vehicle power cabin is divided into an open power cabin and a closed power cabin according to the structure. The open power cabin, that is, the power transmission device and the radiator fan air duct are in the same space, without isolation. The enclosed power cabin, that is, the power transmission device and the radiator cooling air passage are separated by a partition. Because the enclosed type adopts the external air intake mode, no air enters the outer wall air passage of the power transmission device, resulting in heat accumulation on the surface of the high temperature component, and the temperature is continuously increased, which affects the reliability of the engine and shortens its service life.

In this paper, a three-dimensional model is established for the outer wall surface of the power cabin power transmission device. Based on the computational fluid dynamics (CFD) method, numerical simulation is carried out. For the problem of poor temperature fluidity inside, the hole is opened above the armor plate, and the bleed air fan is installed, and the size, position, number of the fan and the size of the venting slit are analyzed and calculated.

Finally, based on the temperature near the high temperature components, the exhaust temperature, the power of the fan, and the resistance of the air duct as the evaluation index, the comprehensive evaluation model of the air duct is established, which provides reference and guidance for the comprehensive evaluation of the outer surface air passage of the power transmission device [3].

2. PROPERTIES

2.1 Establishment of geometric models lanning

In this paper, the power cabin is modeled according to the actual vehicle ratio application software SolidWorks. Since only the outer wall air duct of the power transmission device is considered in this paper, the radiator fan air duct is omitted. The geometric model is simplified, retaining the basic shape of the power transmission device, neglecting some small irregularities and parts with less influence on the flow. Figure 1 is a geometrical diagram of a closed power pod, and Figure 2 is a simplified three-dimensional model of the power cabin.

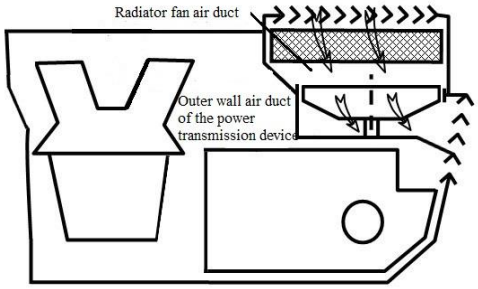

Fig 1. Schematic diagram of a closed power cabin.

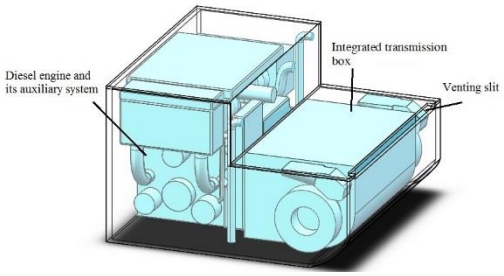

Fig 2 Three-dimensional calculation model of the power cabin.

2.2 Establishment of mathematical model

This paper mainly analyzes the resistance and heat flow field on the air side of the outer wall of the power transmission device. The flow and heat transfer are complicated. Therefore, it is assumed that the air in the cabin is incompressible and constant, and the flow state in the cabin is turbulent and coupled with the wall. Then the governing equation of the fluid satisfies the three major equations of fluid mechanics, namely the continuity equation, the momentum equation and the energy equation.

The turbulence model adopts the standard k-ε model, which is the main turbulence model in engineering flow field calculation. Its computational convergence and accuracy are in line with engineering calculation requirements. Its formula is as follows:

$$\frac{\partial}{\partial x_{\mathrm{i}}}\left(\rho k u_{\mathrm{i}}\right)=\frac{\partial}{\partial x_{\mathrm{i}}}\left[\left(\mu+\frac{\mu_{\mathrm{t}}}{\sigma_{\mathrm{k}}}\right)\frac{\partial k}{\partial x_{\mathrm{i}}}\right]+G_{\mathrm{k}}-\rho\varepsilon \tag{1}$$

Energy Dissipation Rate Equation for Turbulent Flow:

$$\frac{\partial}{\partial x_{\mathrm{i}}}\left(\rho\varepsilon u_{\mathrm{i}}\right)=\frac{\partial}{\partial x_{\mathrm{i}}}\left(\left(\mu+\frac{\mu_{\mathrm{t}}}{\sigma_{\varepsilon}}\right)\frac{\partial\varepsilon}{\partial x_{\mathrm{i}}}\right)+c_{1\varepsilon}\frac{\varepsilon}{k}G_{\mathrm{k}}-c_{2\varepsilon}\rho\frac{\varepsilon^{2}}{k} \tag{2}$$

Where ρ is the density of the fluid, x_i , x_j is the Cartesian coordinate component, k is the turbulent kinetic energy, μ is the viscosity coefficient of the fluid molecule, μ_i is the turbulent viscosity coefficient. ε is the turbulent dissipation rate, σ_k is the turbulent Prandtl number of k , $c_{1\varepsilon}$ and $c_{2\varepsilon}$ are constant coefficients, σ_ε is the turbulent Prandtl number of ε , G_k is the increment caused by the time-averaged velocity gradient k and:

$$G_k=\mu_t\frac{\partial u_j}{\partial x_i}\left(\frac{\partial u_j}{\partial x_i}+\frac{\partial u_i}{\partial x_j}\right) \tag{3}$$

2.3 Meshing

Because the calculation model is more complicated and the flow conditions of its components are different, this paper divides the calculation area into three parts, namely the power cabin outer flow field, the inner flow field, the armored solid domain and mesh division by software ICEM CFD. The theory of the flow field outside the power cabin can be infinite, comprehensive computer performance and calculation accuracy, and finally determine the external flow field size is 4500 × 4000 × 2500 mm, using structured grid division, using unstructured grid for the inner flow field and the armored solid domain. Can adapt to its internal complex shape. The power compartment calculation area grid division diagram is shown in Figure 3.

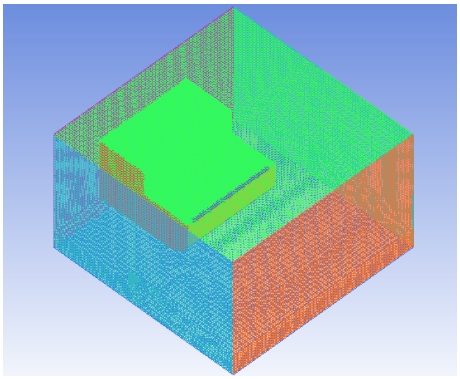

Fig 3 Schematic diagram of calculation grid.

2.4 Boundary conditions

At the entrance of the external flow field, the velocity inlet boundary condition is adopted, and the outlet adopts the pressure outlet boundary, and the left, right and top sides of the calculation area are

set as symmetrical boundary conditions, so that a better convergence effect can be obtained, and the deck surface of the power cabin is obtained. The outer wall surface of the power transmission device is set as a solid wall boundary condition, and the inner and outer wall surfaces of the armor plate are subjected to a fluid-solid coupling heat transfer method as an internal condition, and the outer wall surface of the power transmission device adopts a first type of thermal boundary condition. The wall temperature of the power unit and its auxiliary system can be referred to the literature [4]. The transmission is equipped with a new integrated transmission box, and the situation is complicated. The direct temperature given in this paper is 333K. In addition, the model also considers the effects of solar radiation, ie, armored vehicle orientation, latitude and longitude, date and weather conditions to simulate the heat flux generated by solar radiation on the armor plate and coupled to the Fluent calculation through the source term in the energy equation.

3. ANALYSIS OF CFD CALCULATION RESULTS

The working conditions in this paper are: engine speed is 2000r/min, ambient temperature is 300K, and the vehicle speed is 72km/h.

Figure 4 is a velocity nephogram at Z=1.8m It can be seen from the Figure that the flow velocity in the closed air duct is basically zero, mainly natural convection. This is because the enclosed power compartment adopts the external air intake mode, and there is no cooling air entering the outer wall air passage of the power transmission. Only the tailing deck has a venting slit, which cannot circulate the air inside the cabin. This also causes the surface temperature of the hot parts to accumulate and the heat cannot be taken away.

Figure 5 is a Nephogram of temperature field at Y=0.29m. From this Figure, it can be seen that the temperature above the diesel engine is higher, up to 700K, appearing on the exhaust pipe wall.

Figure. 6 is a temperature field cloud diagram at the cross section of Y=0.29m. This area is located directly above the exhaust pipe, and the cross-section arrangement is more complicated. From the upper side to the lower side of the screenshot, there are air filters, superchargers and supercharger accessories. , water tanks and other components, and closer to the exhaust pipe, resulting in a higher overall temperature of the area, should be concerned.

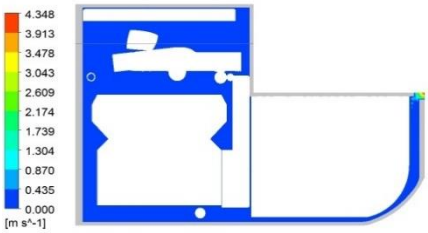

Fig 4 Velocity Nephogram at Z=1.8m

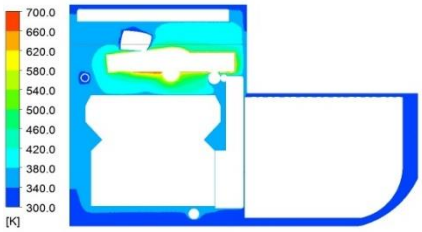

Fig 5 Nephogram of temperature field at Z=1.8m

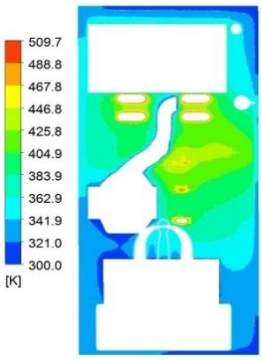

Fig 7 Nephogram of temperature field at Y=0.29m

From the above calculation results, the temperature in the power cabin is generally high, and the no-ventilation structure takes away the heat of the surface of the high-temperature component, which becomes a "dead cavity". In the long run, it will definitely reduce the reliability of diesel engines and affect the life of electronic components in the cabin. Therefore, structural improvements to the power module are necessary.

4. ANALYSIS OF CFD CALCULATION RESULTS

4.1 Improve proposals

Considering the structure and heat dissipation requirements of the power cabin, it is proposed to open the air inlet and increase the air induction fan on the upper armor above the air filter. The air in the cabin is allowed to flow. Achieve the purpose of reducing the heat in the cabin. A schematic diagram of the improvement of the upper deck of the power cabin is shown in Figure 7.

At the same time, due to the addition of the fan, the original flow field outside the power cabin needs to be adjusted. After repeated debugging, the size is determined to be 5500×4000×2800mm. For the fan boundary, the Multiple Reference Frame mode is used. Given the rotation axis and the rotation origin, the direction of rotation is determined by the right-hand rule.

4.2 Improved result analysisimprove proposals

It is still calculated according to the given conditions in the third section, and the fan speed is set to 4600r/min.

Affected by the structure of the power cabin itself, the fan is mounted on the armor panel on the air cleaner side, and this side is defined as the left side. It can be seen from Figure. 8 that the flow velocity on the left side is large, up to 5 m/s, and the cooling effect is good. Part of the air flows into the upper side of the diesel engine, which can take away the heat from the exhaust pipe and the turbocharger to achieve a cooling effect. For the right side, the air flow rate is slower and the cooling effect is not as good as the left side, but the main components on this side are the water tank, one side of the diesel engine and the integrated gearbox, and the heat accumulation is not as serious as the left side.

Comparing Figures 5 and 9, we can see that the temperature in the vicinity of the exhaust pipe and the diesel engine is significantly lowered, and the temperature at a relatively long distance is also improved. Comparing Figure 10 and Figure 6, it can be seen that the temperature in the high temperature region above the exhaust pipe and near the supercharger is reduced from the original 400-450K to 340-380K. And the high temperature area is also significantly reduced.

It can be seen that, after adding the fan, the temperature in the vicinity of the high temperature component is well cooled, the local heat accumulation is basically eliminated, and the distribution of the temperature field becomes more uniform.

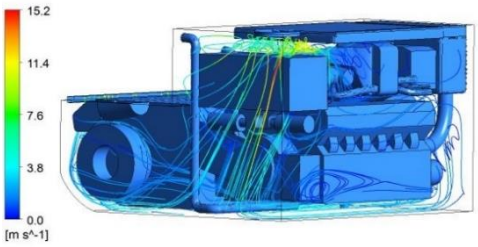

Fig. 8 The improved airflow traces in the cabin

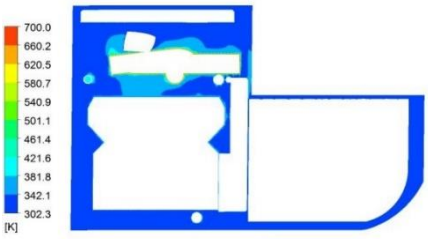

Fig 9 Velocity Nephogram at Z=1.8m section after improvement

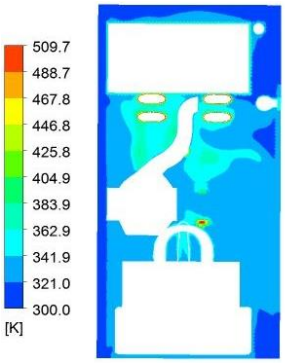

Fig 10 Nephogram of temperature field at Y=0.29m after improvement

Table 1 Optimization plan.

scheme	adjustment
scheme 1	Original scheme
scheme 2	Fan diameter increased by 10mm
scheme 3	Fan diameter increased by 20mm
scheme 4	Fan position forwards 150mm
scheme 5	Fan position moved back 150mm
scheme 6	Power cabin exhaust slit widened by 10mm
scheme 7	Add a small fan to the rear of the fan

4.3 Establishment of Optimized Scheme

Based on the improved scheme, the power cabin cooling components can be appropriately adjusted within the space allowable range to obtain a better solution. In the optimization process, it is difficult to achieve simultaneous optimization between targets. Sometimes the optimization objectives may

contradict each other. Therefore, this paper intends to establish a comprehensive evaluation plan for the power cabin. The optimization plan is shown in Table 1, and the comprehensive evaluation plan is detailed in the next section.

5. ESTABLISHMENT AND ANALYSIS OF COMPREHENSIVE EVALUATION MODEL FOR POWER CABIN

In order to evaluate the various optimization schemes of the outer wall air duct of the power cabin power transmission objectively, fairly and reasonably, and to select the optimal layout scheme, the indicators must be quantitatively evaluated [5]. In this paper, we use the combination of entropy method and subordination degree linear weighted programming method. To determine the weight of each index and comprehensively sort the various programs.

5.1 Establishment of evaluation indicators

Establishing evaluation indicators is a prerequisite for comprehensive evaluation and an important factor affecting evaluation results. In this paper, by consulting related books and combining the cabin cooling requirements, the average surface temperature of the high temperature parts, the air duct resistance, the power of the fan, and the average air temperature at the outlet of the exhaust seam are established as evaluation indexes. These four indicators are very small indicators, that is, we expect the value to be as small as possible. The specific evaluation index system is shown in Figure 11.

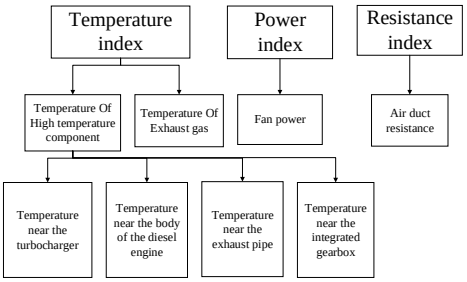

Figure 11. Specific evaluation index system

5.2 Comprehensive evaluation model

5.2.1 Establish underlying indicator weights

It can be seen from Figure 11 that there are four bottom-level indicators under the temperature index of the high-temperature components in the power cabin. This paper mainly uses the entropy method to establish the weight of the four indicators. The entropy method is a commonly used objective weighting method, which can judge the weight according to the observed data difference of each index, and is not affected by subjective factors. Specific steps are as follows.

There are n schemes, m indicators, then fij is the data of the j-th indicator of the i-th scheme (i=1, 2...n; j=1, 2...m), and the j-th index is calculated. The proportion of the i-th plan value to the indicator is as follows:

$$p_{ij} = \frac{f_{ij}}{\sum_{j=1}^{n} f_{ij}} \tag{4}$$

Where Pij is the proportion of the i-th indicator under the j-th evaluation scheme. The Entropy value of item j index:

$$e_j = -\frac{1}{\mathrm{In}n}\sum_{j=1}^{n}\left(p_{ij}\mathrm{In}p_{ij}\right) \tag{5}$$

Where n is the number of schemes:

Calculate the information entropy redundancy (difference) as:

$$d_j = 1 - e_j \tag{6}$$

The weight value of each indicator is:

$$w_{j=}\frac{d_j}{\sum_{j=1}^{m} d_j} \tag{7}$$

5.2.2 The establishment of the weight of the total index and the ranking of comprehensive evaluation

Using the subordination degree linear weighted p method to construct the relative superiority matrix of indicators, determine the four general indicators, namely the temperature near the high temperature components, the temperature of the exhaust seam, the power of the fan, the weight of the air duct resistance, and then the weight of the temperature index of the high temperature component. The proportions obtained by the entropy method are assigned to the various underlying indicators, and finally the comprehensive ordering is performed.

This paper is mainly for the minimum value indicator, and its relative superiority is:

$$\mu_{ij} = (t_{i\max} - f_{ij}) / (t_{i\max} - t_{i\min}) \tag{8}$$

Where:

$$\begin{cases} t_{i\max} = \max\limits_{1\le j\le n}\{f_{ij}\} \\ t_{i\min} = \min\limits_{1\le j\le n}\{f_{ij}\} \end{cases} \tag{9}$$

The index weight can be calculated by the following formula:

$$w_i = \sum_{j=1}^{n}\mu_{ij} / (\sum_{i=1}^{p}\sum_{j=1}^{n}\mu_{ij}) \tag{10}$$

The available relative weighted composite value of the available $x_i \in X$ index is as follows:

$$L_j(w) = \sum_{i=1}^{m} w_i u_{ij} \tag{11}$$

Where Lj is the relative superiority linear weighted comprehensive evaluation value of the power cabin j scheme, and the closer the value of Lj is to 1, the higher the comprehensive capability of the scheme.

5.3 Example calculation

$$p_{ij} = \begin{bmatrix} 0.1427 & 0.1426 & 0.1428 & 0.1431 \\ 0.1426 & 0.1421 & 0.1421 & 0.1430 \\ 0.1424 & 0.1417 & 0.1411 & 0.1428 \\ 0.1444 & 0.1441 & 0.1448 & 0.1433 \\ 0.1426 & 0.1434 & 0.1442 & 0.1424 \\ 0.1422 & 0.1435 & 0.1435 & 0.1429 \\ 0.1430 & 0.1426 & 0.1415 & 0.1424 \end{bmatrix}$$

Then use Equation 5 to Equation 7 to get the weight of the four underlying indicators to be w= (0.1558 0.2192 0.5891 0.0359).

For the four general indicators, first use Equation 8 to establish the superiority equation as follows：

$$\mu = \begin{bmatrix} 0.5947 & 0.0000 & 0.9501 & 0.6597 \\ 0.8096 & 0.1660 & 0.4963 & 0.0881 \\ 1.0000 & 1.0000 & 0.0000 & 0.0000 \\ 0.0000 & 0.0124 & 0.8504 & 0.0375 \\ 0.5925 & 0.7054 & 1.0000 & 0.8854 \\ 0.4605 & 0.2573 & 0.8978 & 1.0000 \\ 0.8561 & 0.9668 & 0.7556 & 0.3905 \end{bmatrix}$$

Using Equation 10, the weight of the four items is w= (0.2795 0.2014 0.3208 0.1984). The weight index for the temperature near the first high temperature component is replaced by four high temperature indicators, and the final weight is obtained by proportional distribution. w= (0.0435 0.0613 0.1646 0.0100 0.2014 0.3208 0.1984).

Table 2 Comprehensive evaluation results.

Scheme	Comprehensive evaluation value	Sort
1	0.6000	4
2	0.4247	6
3	0.4724	5
4	0.2827	7
5	0.7297	2
6	0.6596	3
7	0.7398	1

Finally, Equation 11 is used to calculate the comprehensive evaluation values of seven schemes as shown in Table 2.

It can be concluded from the above that the comprehensive evaluation value of the scheme 7 is the highest, that is, a smaller fan is added after the fan, although the fan power and the air duct resistance are slightly increased, but the cooling effect is more obvious, so the overall performance is optimal. Both scheme 2 and scheme 3 increase the diameter of the fan, but its cooling effect is not good, but it will increase the power of the fan and the air duct resistance, so it is not as good as the original scheme. Scheme 4 and scheme 5 move the fan forward and backward respectively. It can be seen that the backward migration scheme is better than the original scheme, and the evaluation value of the forward migration scheme is lower than the original scheme. Scheme 6 widens the venting slit, resulting in a decrease in air duct resistance. And its comprehensive evaluation value is higher than that of scheme 1.

6. CONCLUSION

In this paper, the heat flow field of the enclosed power module is studied, and its structure is improved. Seven optimization schemes are proposed, and a comprehensive evaluation model is established to sort the schemes. The conclusions are as follows:

(1) The temperature in the power cabin of the original structure is generally high, which will affect the reliability of the components inside. After the structural improvement, the temperature field and flow field in the power cabin are significantly improved.

(2) The comprehensive evaluation model is established by the combination of entropy method and subordination degree linear weighted programming method. The evaluation index system is established, and then the seven schemes are sorted. It can be concluded that the comprehensive evaluation value of scheme 7 is the highest.

(3) The comprehensive evaluation model proposed in this paper can provide an effective evaluation method for the formulation of the power cabin, and has a high degree of credibility.

REFERENCES

[1] Li, H. J., Bi X. P., 2004, Integrated Evaluation on Themral Working Condition in Tank Power Cabin Based on the Themral Charge Value Method. Journal of Academy of Armored Force Engineering, 18(01): 62-65.

[2] Liu, X. X., Cao Y.K., BI, X, P., 2007, Review of Research on Air Flow and Heat Transfer inEngine Compartment of Tank. Acta Armamentari, 28(08): 1011-1016.

[3] Zhang, J. X., 2000. High mobility mobile vehicle power system. China Science and Technology Press, Beijing. 2nd edition.

[4] Luo, Q. G., Lu, J., Zhao, Y., Gui, Y., 2019. Simulation Analysis of One-Dimensional Heat Transfer of Diesel Engine Based on GT-SUITE. Journal of Ordnance Equipment Engineering, 40(06): 206-210.

[5] Bi, X. P., Lv L.D., Z, G, Y., 2012. Evaluation of Cooling Air Duct Comprehensive Performance in Vehicle Based on CFD Analysis. Chinese Internal Combustion Engine Engineering, 33(03): 49-53.